Supporting Information

Preparation of Porous Reduced Graphene Oxide using Cellulose Acetate for High Performance Capacitive Desalination

*Penghui Wang, Guoqian Lu, Huan Yan, Wei Ni, Min Xu, Yifei Xue, Yi-Ming Yan**

School of Chemical Engineering and Environment, Beijing Institute of Technology, Beijing, 100081, People's Republic of China

Experimental Section

Material: Graphite powder (200 mesh 99.9%) used in all experiments was purchased from Alfa Aesar (China) Chemical Co., Ltd. Carbon paper was purchased from hesen Electric Co., in Shanghai, China. Ethanol (99.7%) was purchased from Beijing Reagent Company. Sulphuric acid (98%), HCl acid (37%) and H_2O_2 (30%) Ascorbic acid (AR), N-methyl pyrrolidone (AR), $KMnO_4$ powders (AR), Sodium powders (AR), Cellulose Acetate (AR), were purchased from Beijing Chemical Works. All water mentioned in this paper was deionized water.

Synthesis of the CA-RGO and RGO: The graphite oxide (GO) was synthesized from natural graphite flake by a modified Hummers method. Then the preparation of graphene oxide (GO) was dispersed in 80 ml of N-methyl pyrrolidone and get the mixed solution. Then 800 mg of Cellulose Acetate (CA) and 80 mL of DI water were added into the mixture, and the mixture was ultrasonicated for 30 min in the cell crusher. After that, the sample was dispersed in boiling water and reduced by adding 400 mg of ascorbic acid into the solution under ultrasonication for 30 mins. The

sample was further treated by 24 h dialysis before submitted for freeze drying. Finally, the obtained material was dried in the tube furnace (200 ℃ for 2 h). The sample was defined as CA-RGO. The RGO sample was prepared by following the same procedure except that no surfactant was used.

Material Characterization: The surface morphology and structure of the as-synthesized samples were examined by using SEM with energy spectrum analysis (two FEG 250), all of the test results was performed at a beam voltage of 20 kV. And high magnification morphology was examined by the Japanese electronic (JEOL JEM-2100-type transmission electron microscope (TEM), which the working voltage is 100 kV. Sample macro morphology is obtained by Nikon photo. The pore size distribution and Brunauer-Emmet-Teller (BET) specific surface area were deduced from the nitrogen physical adsorption measurement data obtained using an Autosorb-IQ2-MP-C system, and the pore size distribution was derived from the adsorption branches of the isotherms using the Barrett-Joyner-Halenda (BJH) model. X-ray diffraction (XRD) spectra were acquired using a Rigaku tall Ultima IV. Raman spectra were recorded with a RM 2000 Raman spectroscopy tester produced by the British Renishaw, which A He-Ne laser (633 nm) was used as the light source for excitation. Fourier transform infrared (FT-IR) spectroscopy data were acquired with a NICOLET IS10 Fourier infrared spectrometer, which scanning spectrum range was 400 ~ 4000 cm^{-1}, with the air as the background. The hydrophilic measured by contact Angle meter (HARKE- SPCA).

Electrode preparation: Electrochemical measurements were performed in three-

electrode cell configuration on electrochemical analyzer (CHI660 instruments) Polytetrafluoroethylene (PTFE, Sigma-Aldrich; 60 wt. % dispersion in water) was added to the mixture of samples and carbon black (samples / carbon black / PTFE = 85:10:5 by weight) as a binder. The working electrode was fabricated by casting the mixture on a carbon paper and drying in 60℃ under vacuum drying overnight. For CDI process, a pairs of electrodes with an equal amount of CA-RGO (or RGO) separated by an insulating spacer was assembled to a home-made CDI unit. The capacitive deionization behavior of SRGO and RGO electrodes were carried out in 25 mL NaCl aqueous solution with an initial conductivity of 106 μS·cm^{-1} and a flow rate of 8 ml·min^{-1}. The applied voltage is set as 1.5 V.

The electrosorption capacity (qe) of per active material cell can be calculated using Equation (2) while the deionization efficiency (ηd) can be calculated using Equation (3).

$$q_e = \frac{V_{olume}(C_{eff} - C_0)}{w} \tag{2}$$

$$\eta_d(\%) = (1 - \frac{C_{eff}}{C_0}) \times 100 \tag{3}$$

Where *v* is the scanning rate; *w* is the quality of the active materials; Va and Vc represent charging and discharge voltage respectively; I refers to current, and *V* is voltage; Volume is the volume of NaCl solution and C0 is the initial concentration; C_{eff} is the lowest concentration at adsorption equilibrium.

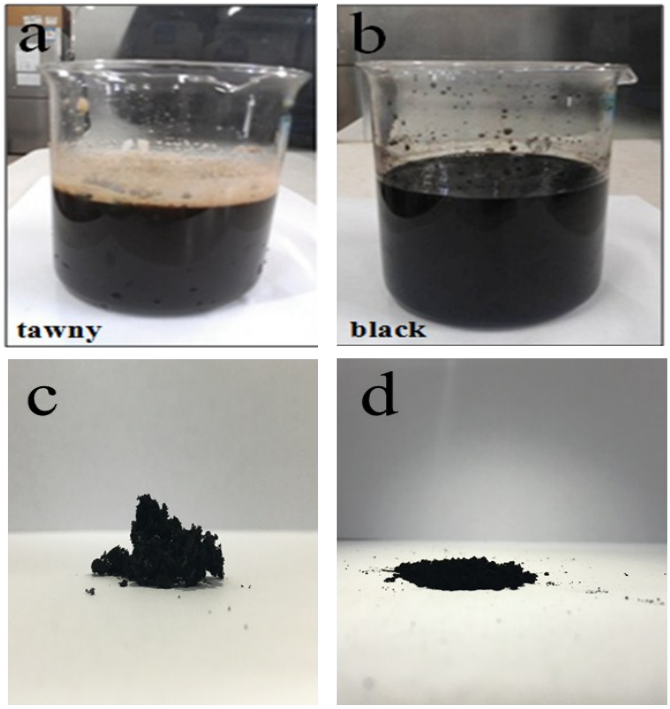

Fig.S1 Photo images of (a) CA-RGO solution before reducing; (b) Solution of CA-RGO after half reducing;(c) CA-RGO powder; (d) RGO powder.

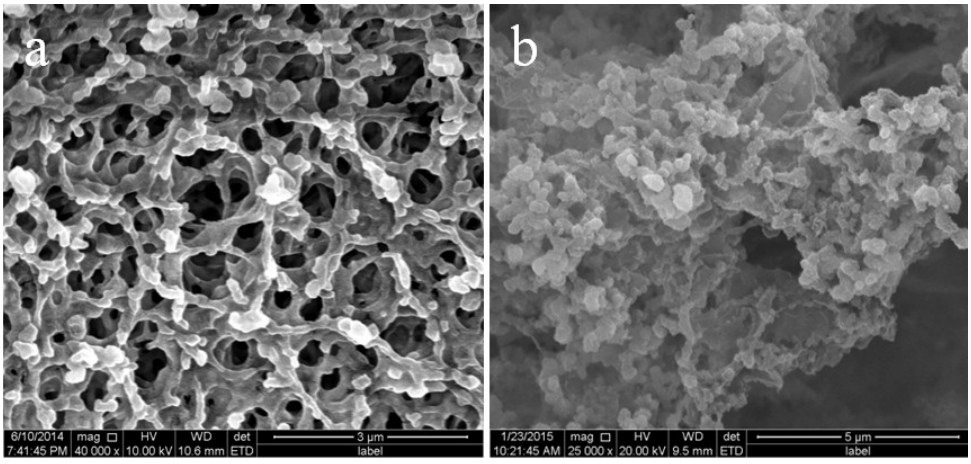

Fig.S2 SEM images of (a) cellulose acetate skeleton obtained with phase inversion method; (b) graphene oxide adhered on cellulose acetate skeleton.

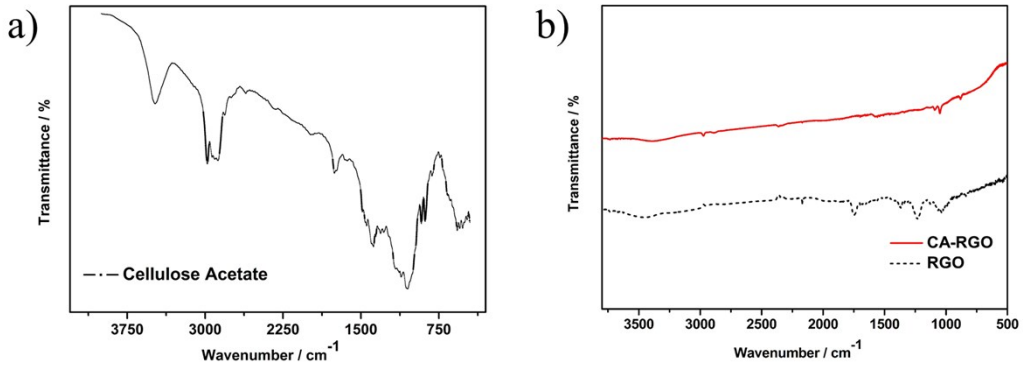

Fig. S3 (a) FT-IR spectra of cellulose acetate; (b) FT-IR spectra of CA-RGO and RGO.

Table S1 Comparison of electrosorption capacity obtained with different carbon electrode materials

Electrode [units]	Electrosorption capacity (both electrodes) [mg g^{-1}]	Specific surface area [m^2 g^{-1}]	Initial solution concentration [μ S/cm]	Applied voltage [V]	Reference
GN	1.85	14.2	50 μ S/cm	2	[S1]
3DHPC	2.16	1036.8	65 μ S/cm	2	[S2]
GE/MC	0.731	624.7-677.3	89.5 μ S/cm	2	[S3]
ACF/CB	1.99	917	197 μ S/cm	1.6	[S4]
STGS	4.95	305	106 μ S/cm	1.5	[S5]
NG	4.81	358.9	100 μ S/cm	1.8	[S6]
PG	3.85	154.7	100 μ S/cm	1.8	[S6]
Gr/SnO_2	1.49	---	61 μ S/cm	1.4	[S7]
CNTs-RGO	0.5-1.4	438.6	100 μ S/cm	1.2	[S8]
RGO/PANI	1.56	-----	58.9 μ S/cm	2	[S9]
OMC/CNT	0.63	864.5	93.5 μ S/cm	1.2	[S10]
GHMCSs	2.3	400.4	68.5 μ S/cm	1.6	[S11]
GNS	4.1	464	500 μ S/cm	1.2	[S12]
3DMGA	1.97-5.39	339	108.6 μ S/cm	1.2-2	[S13]
OMCs	3–4.5	700--1400	1078 μ S/cm	1.2	[S14]
GR/CNT	1.41	365.1-479.5	57 μ S/cm	1.0	[S15]
CA-RGO	5.56	378.4	106 μ S/cm	1.5	This work

Reference

[S1] H.B. Li, T. Lu, L.K. Pan, Y. P. Zhang and Z. Sun. *J. Mater. Chem.* **2009.** 19, 6773–6779.

[S2] X.R. Wen, D.S. Zhang, L.Y. Shi, T.T. Yan, H. Wang and J.P. Zhang. *J.mater.chem,* **2012,** *22*(45), 23835-23844.

[S3] Z. Dengsong, W. Xiaoru, S. Liyi, Y. Tingting & Z. Jianping. *Nanoscale,* **2012**, *4*(4), 5440-6.

[S4] W. Gang, D. Qiang, L. Zheng, P. Chao, Y. Chang and Q. Jieshan. *Journal of Materials Chemistry,* **2012,** *22*(41), 21819-21823.

[S5] Z.Y. Yang, L.J. Jin, G.Q. Lu, Q.Q. Xiao, Y.X. Zhang, L. Jing, X.X. Zhang, Y.M. Yan, K.N. Sun. Advanced Functional Materials, 2014, 24(25): 3838-3838.

[S6] X. Xu, L. K. Pan, Y. Liu, T. Lu, Z. Sun. *Journal of Colloid & Interface Science*, **2015**, 445:143-150.

[S7] A.G. El-Deen, N.A.M. Barakat, K.A. Khalil, M. Motlak, H.Y. KimA. *Ceramics International,* **2014**, 40(9):14627-14634.

[S8] H. Li, S. Liang, J. Li, L. He. *J.mater.chem.a,* **2013,** 1(1), 6335-6341.

[S9] Y. Zhang, L. Zou, Y. Wimalasiri, J.Y. Lee, Y. Chun. *Electrochimica Acta*, **2015**, 182:383-390.

[S10] P. Zheng, D.S. Zhang, L.Y. Shi, T.T. Yan, S. Yuan, H.R. Li, R.H. Gao, and J.H. Fang. *Journal of Materials Chemistry,* **2012**, 22(14):6603-6612.

[S11] H. Wang, L. Shi, T. Yan, J. Zhang, Q. Zhong, D. Zhang, *J. Mater. Chem. A*, **2014**, 2:4739.

[S12] B. Jia, L. Zou. *Chemical Physics Letters,* **2012**, 548(4), 23–28.

[S13] H. Wang, D.S. Zhang, T.T. Yan, X.R. Wen, J.P. Zhang, L.Y. Shi and Q.D. Zhong. *J.mater.chem.a,* **2013,** *1*(38), 11778-11789.

[S14] F. Duan, X. Du, Y. Li, H. Cao, Y. Zhang. *Desalination*, **2015**, 376:17-24.

[S15] D.S. Zhang, T.T. Yan, L.Y. Shi, Z. Peng, X.R. Wen and J.P. Zhang. *Journal of Materials Chemistry,* **2012,** *22*(29), 14696-14704.